JOURNAL OF MATERIALS SCIENCE 8 (1973) 676–687

Fatigue behaviour of ribbon-reinforced composites

E. ANDERSON
Battelle, Geneva Research Centre, 7, route de Drize, CH—1227 Carouge/Geneva

The fatigue behaviour of aluminium-based composites reinforced with high-strength steel ribbons has been examined. In the directions both parallel (longitudinal composites) and perpendicular (transverse composites) to the principal ribbon axis the development of the fatigue deformation is controlled by the matrix. The steel-matrix bond does not deteriorate during the initial stages of fatigue. The fatigue limit at 10^7 cycles was arbitrarily defined in the case of the longitudinal composites as corresponding to approximately the half-destruction of the composite. In this way the limit for a composite with a volume fraction, V_r of 0.25 was around 25% of the fracture strength while with a V_r of 0.34, the limit was raised to about 33% of the fracture strength. The use of an alloy matrix increases the fatigue strength of the composite. The fatigue mechanism in both longitudinal and transverse composites initially involves matrix cracking; this leads to steel-aluminium or aluminium-aluminium debonding parallel to the principal stress axis in specimens fabricated from pre-coated steel ribbons, followed by ribbon fracture. In specimens fabricated by simply rolling together the steel ribbons and aluminium foils, little debonding is evident. The debonding results in a high fracture resistance.

1. Introduction

In previous publications [1, 2], the mechanical properties and deformation mechanisms of aluminium reinforced with steel ribbons, were presented. The present communication deals with the fatigue behaviour of these composite materials. The interest in ribbon-reinforced composites lies in the increased transverse strengthcompared to unidirectionally-reinforced filamentary composites. This increase in transverse characteristics is also apparent in the fatigue behaviour.

The reinforcements obtained with high strength steel ribbons can be predicted on the basis of rule-of-mixtures equations analogous to those derived for continuous and discontinuous filament reinforcement. In the direction parallel to the principal ribbon axis (longitudinal composites), the tensile strength, σ_L of a composite containing a volume fraction, V_r of ribbons is given by the following relation:

$$\sigma_L = \sigma'_M (1 - V_r) + \sigma_r V_r$$

where σ_r is the fracture strength of the ribbons, and σ'_M the stress on the matrix at composite fracture.

In the direction perpendicular to the principal ribbon axis (transverse composites), the tensile strength, σ_c of a composite is given by

$$\sigma_c = \sigma'_M (1 - V_r) + \sigma_r V_r \left(1 - \frac{1 - \beta}{W/W_c}\right)$$

where β is a constant $\simeq 0.5$, W is the ribbon width, and W_c is the critical ribbon width necessary for the transfer of stress from the matrix to the ribbon.

This critical width depends on the fracture strength of the ribbon, σ_r, the shear strength, τ of the matrix at the matrix-ribbon interface, according to the following relation:

$$\frac{W_c}{t} = \frac{\sigma_r}{\tau}$$

where t is the ribbon thickness.

Some recent work has shown theoretically [3-5] and experimentally [6] the utility of employing ribbon-shaped "filament" reinforcement to develop high transverse strengths which, with wide ribbons, may even approach the

longitudinal strengths. An extremely important theoretical prediction [5] was that the elastic modulus in the transverse direction would approximate that in the longitudinal direction, a prediction which has been verified experimentally in the course of the present research [1].

Although the strength characteristics of fibre-reinforced metal–matrix composites have received a great deal of attention both theoretically and experimentally, the fatigue behaviour is less well documented. Forsyth *et al* [7] were among the first to find that a considerable reduction in the rate of fatigue crack propagation resulted from the addition of 13 vol % of continuous steel filaments to an aluminium matrix. This effect was attributed to the high resistance to cracking of the steel filaments.

Baker [8-10] has studied in detail the reverse bend fatigue behaviour of aluminium-stainless steel filament-reinforced composites and concluded that for continuous fibres [8, 9], increasing volume fraction increased fatigue life, apparently by reducing the plastic strain range of the matrix during the cycling; fatigue failure occurred mainly by a process of fibre–matrix interfacial crack propagation; specimens exhibiting limited intermetallic formation at the aluminium-steel interface had greater fatigue resistance than composites showing no intermetallic formation.

For discontinuous fibres [10], the conclusions were that the fatigue properties depend strongly on the fibre length, even after account has been taken of the plastic strain range of the matrix. In addition to the failure processes encountered in specimens reinforced with continuous fibres, fatigue damage occurred at fibre ends near the specimen surfaces, thus, in this case, it is even more important to have strong interfacial bonding; the fatigue resistance increases with increasing fibre length–the shorter the fibre, the more numerous the fibre ends and the higher the probability of a continuous easy crack path through the specimen.

In push-pull experiments on aluminium-steel composites, Varschavsky and Tamayo [11] also found that the fatigue properties were improved by improving the fibre–matrix bond. The results would seem to indicate that the fatigue resistance of composites in push-pull is higher than in reverse bend. The fatigue damage during reverse bend tests on stainless steel filament-reinforced aluminium was accompanied by a change in flexural modulus [8], while boron-reinforced aluminium did not show this effect [12]. In the latter case no fibre degradation was apparent up to final failure while in the former example gradual failure of the steel filaments took place.

Boron-reinforced 6061 aluminium alloy exhibits increasing fatigue resistance with increasing volume fraction of filaments [13]. Final failure was again catastrophic. Increased fatigue resistance of boron composites was obtained by decreasing the work-hardening rate of the aluminium alloy matrix [14]. This suggests that the behaviour of the matrix controls the fatigue behaviour of the composite. The failure mechanism proposed, however, involves the build-up of stress concentrations in the matrix at points of initial filament fracture (due to fabrication, for example) to a stress level capable of fracturing neighbouring filaments; final composite fracture follows close on this event.

Hancock [15] has recently studied the behaviour in axial fatigue of aluminium reinforced with beryllium wires and concluded that the crack-growth resistance of the matrix was of major importance in determining the fatigue life. At low strain ranges, failures proceeded by filament fracture and interface cracking, final fracture involving the shearing of the aluminium matrix. At high strain ranges, cracks grew directly across the matrix with little interfacial crack growth.

2. Composite fabrication

The high-strength steel ribbons used in the composite preparation were 0.06 mm thick and 3, 4 and 8 mm wide. The 3 and 4 mm wide ribbons were pre-coated with aluminium before compaction by hot-pressing or hot-rolling with or without aluminium or aluminium-silicon foil, the thickness of which was varied in order to vary the ribbon content of the composites. The 8 mm ribbon composites were fabricated by hot-rolling of uncoated ribbons and aluminium foil.

The steel ribbons employed were:

1. cold rolled 17-7 stainless and maraging (age-hardenable martensitic iron-18% nickel alloy) with strengths of around 180 kg mm^{-2} in the composites;
2. annealed maraging with a strength of around 160 kg mm^{-2} in the composites.

Although the strength of the steel affected the composite strength, the deformation and fracture mechanisms of the composites did not seem

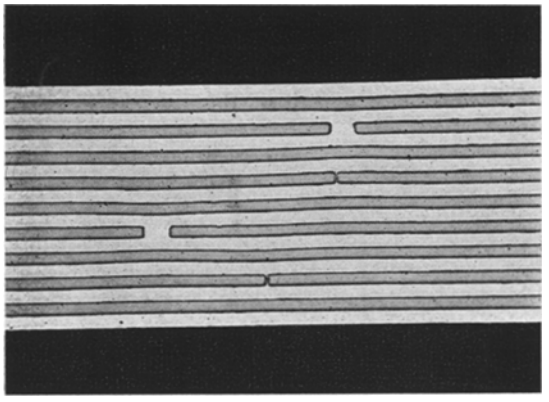

Figure 1 Transverse cross-section of a ribbon composite (×20).

to vary with the type of steel employed. The structure of the composites in the transverse direction was as illustrated in Fig. 1. In the specimens tested in fatigue, six layers of ribbons were incorporated since the composite strength has been found to be virtually independent of the number of layers above six.

3. Mechanical properties

The mechanical properties of the composites have been dealt with in detail in a previous publication [1]. The tensile strengths in the longitudinal and transverse directions follow the rule-of-mixtures equations given previously. In the transverse direction, the tensile strengths increase with ribbon volume fraction and with ribbon width as indicated in Fig. 2. The value of 45 for the critical ratio, W_c/t at room temperature has been calculated by various techniques [1] and has been used in the construction of the straight lines in Fig. 2.

4. Fatigue testing

Standard flat fatigue specimens with a reduced centre section were machined from composite sheets prepared either by hot-pressing or hot-rolling. The tests were performed in reverse bend on a Wöhler machine at frequencies of 25 Hz for low stresses and 10 Hz for high stresses under conditions of alternating stress about a zero strain position. The amplitude was chosen so as to produce a maximum stress at the surface equal to the values of σ_F given in the tables.

The fatigue behaviour did not seem to depend on the technique of fabrication, provided that perfectly compacted specimens were obtained.

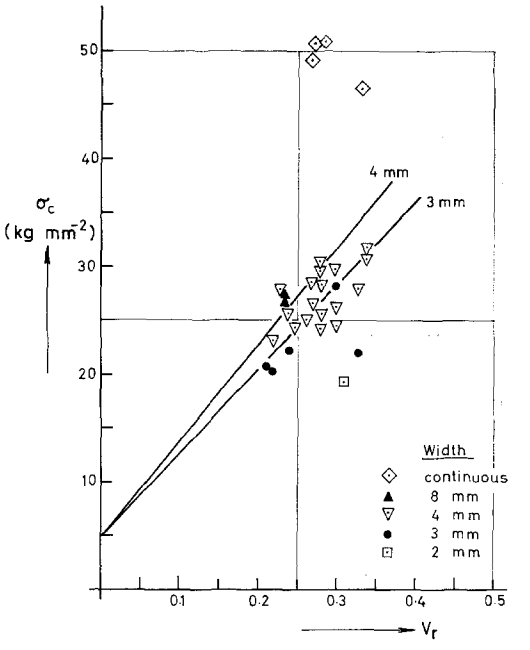

Figure 2 Fracture strength of composites, σ_c as function of the volume fraction, V_r at room temperature. Lines drawn for $W_c/t = 45$.

In addition, the hot-rolling procedure provided large, uniform composite sheets on which a comprehensive study could be carried out.

As the fatigue damage in the specimen progressed the modulus (i.e., the deflection stress) gradually decreased. Thus, during the tests the machine was stopped when the deflection stress had dropped to about 80% of its initial value; before continuing the test the deflection stress was increased to the initial value. The limit of useful fatigue life was taken as being when the deflection had fallen to at least 40% of the initial value.

The above definition of fatigue limit for the longitudinal composites corresponds approximately to the "half destruction" of the composite, since approximately 50% of the tensile strength remains after such a fatigue test. The fatigue limit of composites containing ductile filaments is difficult to define since the failure is progressive. In the case of the transverse composites the definition does not correspond to their "half-destruction" since the mechanism of failure involves ribbon pull-out as well as ribbon fracture.

In the course of similar tests on aluminium-boron composites [16], the fatigue limit was

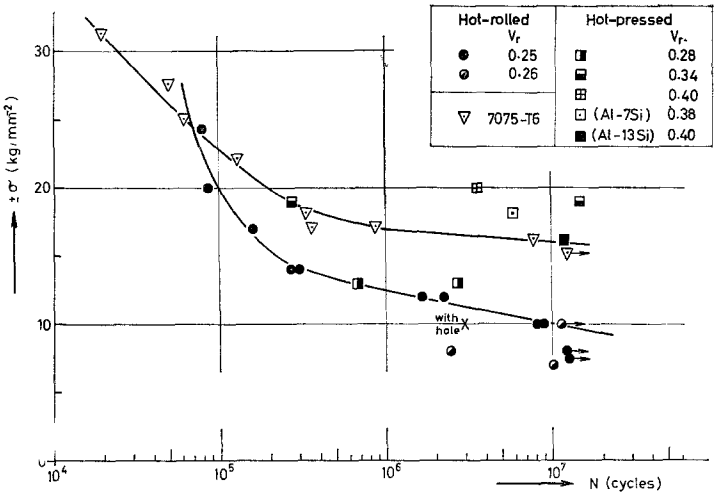

Figure 3 Number of cycles to "failure" as a function of alternating stress for longitudinal aluminium-steel ribbon composites compared with a 7075-T6 aluminium alloy.

defined as being a reduction of 30% in the initial frequency of the test.

5. Fatigue results and discussion of longitudinal composites

5.1. Fatigue limit

The results presented in Table I and Fig. 3 have been obtained on hot-pressed and hot-rolled samples containing 3 and 4 mm wide by 0.06 mm thick ribbons. There does not seem to be an effect of frequency on the fatigue behaviour, so for the high stress ranges a frequency of 10 Hz was chosen in order that the test would not be over in a matter of minutes.

The definition of the end of useful fatigue life for metals and alloys corresponds to final fracture. The definition for the composites chosen in the present work, of the half destruction of the material, has been arrived at by analysing the fatigue mechanism in the composites.

In the composites discussed here, a 2 to 4 μm thick Fe_2Al_5 intermetallic layer was present at the steel-pure aluminium interface and ensured optimal fatigue properties, i.e., no premature interface break-down. In pure aluminium-based specimens not exhibiting an intermetallic layer, the fatigue failure was rapid. Aluminium-silicon matrix composites exhibited no intermetallic at the interface with the steel but bonding and fatigue properties were optimal, and the fatigue mechanism similar to that shown by the pure aluminium matrix composites.

The stress ranges employed greatly exceed the elastic limit of the aluminium or the aluminium-silicon matrix on the outer surfaces on the specimens so that fatigue damage is built up more or less rapidly as a function of the stress level and cracks appear in the matrix, propagating from the outer specimen (aluminium) surface to the steel ribbons. In addition, debonding may take place along the aluminium-aluminium or the aluminium-steel interface whichever is weakest. New fatigue cracks then appear in the aluminium at the free surfaces and propagate towards the steel ribbons.

The aspect of a longitudinal fatigue specimen containing 0.38 volume fraction of steel in an aluminium-7% silicon matrix is shown in Fig. 4 after 5.7×10^6 cycles at an alternating stress of $\pm$ 18 kg mm^{-2}. No ribbon fracture is evident in this section, the specimen degradation mainly taking place by matrix cracking and interfacial debonding.

Fig. 5, which is a detail of the same specimen, shows a ribbon and associated aluminium-silicon matrix which has debonded from the rest of the specimen. The cracks are seen to propagate from the free matrix surfaces towards the ribbon and are deflected along the matrix-steel interface or along the interface between the original matrix coating and the added matrix foils. The matrix fatigue cracking is limited to the matrix surrounding the outer steel ribbons. In the example shown in Figs. 4 and 5, no steel

TABLE I Results of the fatigue tests on longitudinal composites in reverse bend at $\pm\sigma_F$

	Test specimen Volume fraction of ribbons, V_r	Frequency (Hz)	$\pm\sigma_F$ (kg mm^{-2})	Number of cycles N ($\times 10^{-6}$)	$\pm\sigma$ deflection at end of fatigue test (kg mm^{-2})	Tensile strength after test σ_E (kg mm^{-2})	Tensile strength before test, σ_C (kg mm^{-2})	σ_E/σ_C (%)
Hot-rolled specimens pure Al matrix		25	7.0 increased to	10.8	7.0			
			10.0	1.7	6.1	22.5	47.7	47
	0.25	25	10.0	8.9	4.1	25.4	,,	53
		25	12.0	1.6	5.0	20.8	,,	43
		25	14.0	0.26	5.4	20.3	,,	42
		10	14.0	0.26 broken at a defect	5.5	22.4	,,	47
		10	17.0	0.04	2.9	5.8	,,	12
		10	17.0	0.17	3.6	20.4	,,	43
		10	20.0	0.08	6.2	30.3	,,	63
		10	24.4	0.08	7.8	34.5	,,	72
	With a central hole of 2 mm ϕ	25	10.0	3.0	3.4	13.9	,,	29
	0.26	25	10.0 increased to	14.7	10.0	—		
			12.0	0.2	5.2	19.4	54.3	36
	0.25	25	10.0	8.2		31.5	54.0	58
		25	8.0 increased to	11.3	8.0	—		
			12.0	3.0	1.5	11.0	54.0	20
	0.26	25	8.1	2.3	2.4	17.5	44.2	40
		25	7.0	9.7	2.0	18.3	,,	41
Hot-pressed specimens pure Al matrix	0.28	25	10.0	1.1	small	14.1	49.4	28
	0.34	25	19.0	0.27	17.0	56.4	60.0	94
	0.34	25	19.0	17.98	15.0	35.5	60.0	60
	0.28	25	13.0	2.56	10.4	21.8	49.1	44
	0.28	25	13.0	0.69	9.0	49.5	49.1	100
	0.35	25	19.5	0.04	7.0	66.1	63.0	> 100
	0.35	25	19.5	0.02	15.5	65.3	63.0	> 100
	0.40	25	20.0	0.55	15.0	51.7	70.0	74
Hot-pressed specimens	Al-13% Si (0.40) annealed at 420°C for 3 h	25	16.0	11.8	6.0	—	—	—
	Al-7% Si (0.38) annealed at 420°C for 3 h	25	18.0	5.7	9.0	—	—	—

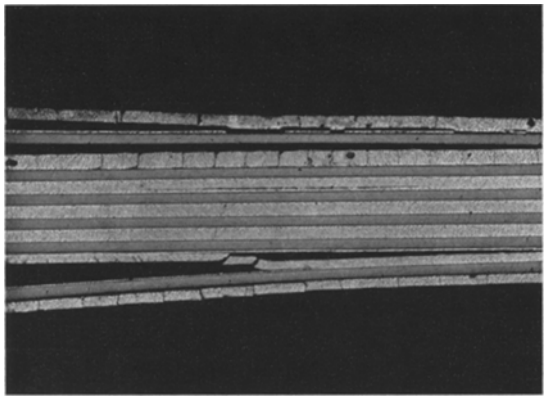

Figure 4 Aspect near centre of longitudinal Al-7% Si matrix composite ($V_r = 0.38$) after 5.7×10^6 cycles at ± 18 kg mm^{-2} ($\times 20$).

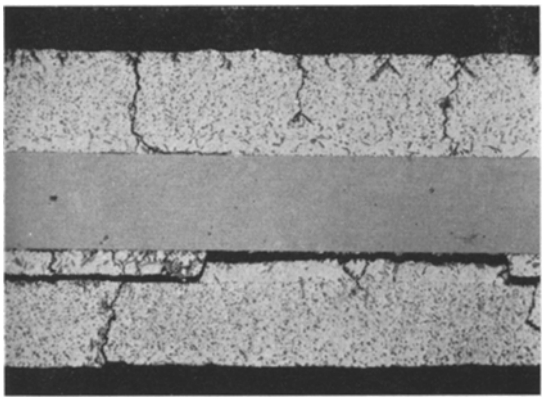

Figure 5 Detail of specimen shown in Fig. 4 ($\times 200$).

ribbon fracture was observed but in the tests carried out to determine the fatigue limit the degradation of the composites led to fracture of ribbons in the two outer layers. At this point the tests were stopped and the number of cycles supported by the composites taken as the useful fatigue life of the composite at the imposed stress level.

Since it is more than likely that other ribbons are broken in the interior of the specimen one can conclude that the tests have been stopped when between 50 and 66% of the mechanical strength of the composites remained (there are six layers of ribbons in the specimens). This conclusion has been confirmed by tensile tests conducted on specimens fatigue tested to this limit: approximately 50% of the mechanical strength remained as is evidenced in Table I. Thus, the S/N curve drawn in Fig. 3 represents, as a function of the number of cycles, the stress necessary to damage to about 50% a composite containing a steel ribbon volume fraction of about 0.25.

In the case of the samples tested at stresses close to the limit (10^6 to 10^7 cycles) the first cracks in the aluminium appeared after about 60% of the total number of cycles. The first ribbons broke after around 80% of the total number. The samples tested at stresses above the limit exhibited matrix cracks already after 10 to 20% of the test duration, but the first ribbons did again not break until after 80% of the total duration.

The high resistance of the ribbon composites to crack propagation is evidenced by the result for a specimen containing a 2 mm diameter central hole. The hole had the effect of reducing the fatigue life at $\pm$ 10 kg mm^{-2} from 9×10^6 cycles to 3×10^6 cycles. The presence of stress concentrations in a high strength aluminium alloy: 7075-T6 leads, on the other hand, to rapid premature failure.

The plastic strain range, Δe_p to which the matrix is subjected in each cycle is given by the following relation [8]:

$$\Delta e_p \simeq \frac{2\sigma_F - (2\sigma_{ym}/E_m)\,[E_r V_r + E_m(1 - V_r)]}{E_r V_r + (\delta\sigma/\delta\epsilon)\,(1 - V_r)} \quad (1)$$

where σ_F is the alternating stress applied to the composite, σ_{ym} the yield stress of the matrix, $\delta\sigma/\delta\epsilon$ the effective modulus of the yielded matrix, V_r the volume fraction of ribbons, and E_m and E_r the elastic moduli of matrix and ribbons respectively.

Applying this relation to the results of Table I shows that a specimen breaks before the fatigue limit at 10^7 cycles if the plastic strain per cycle is greater than about 0.3%. This observation is in close agreement with that of Baker [8] on steel filament-reinforced aluminium and Baker *et al* [17] on boron-aluminium composites and it can be concluded that the matrix fatigue controls the composite fatigue.

5.2. Effect of volume fraction, V_r

All the specimens cut from hot-rolled composites contained around 0.25 volume fraction, V_r of ribbons; two hot-pressed specimens with $V_r = 0.34$ presented higher fatigue resistances than the specimens with $V_r = 0.25$. From the few results obtained so far it seems that the ratio of fatigue

limit to fracture strength increases with volume fraction from 25% for $V_r = 0.25$ to 33% for $V_r = 0.34$. This is a higher ratio than found for aluminium reinforced with steel wires [11] but this may be due to the stronger interfacial bond strength in the present case.

5.3. Effect of the matrix

The results show that although the development of the fatigue deformation is controlled by the matrix, the final fracture is determined the steel ribbon resistance, i.e., the fatigue damage in the matrix leads to crack formation, followed by stress concentration build-up at the steel interface which finally induces interface failure and steel fracture. This is slightly at variance with observations of Varschavsky and Tamayo [11] who, because of poor interfacial bonding in aluminium alloy-steel wire composites, observed the following failure sequence: wire-matrix interface, matrix, and finally the steel wires.

Several studies show that the fatigue strength of composites increases with increasing matrix strength. In aluminium-boron composites [16] the fatigue strength in reverse bend is doubled by employing a 2024 alloy matrix in place of pure aluminium. Equally, in tension-compression tests the fatigue resistance of aluminium-boron composites is strongly dependent on the nature of the alloy of the matrix [14, 18]: with a 6061 alloy matrix the fatigue limit at 10^7 cycles is about twice that with a 2024 alloy matrix [12].

In the present work, the fatigue behaviour of the specimen with $V_r = 0.38$ in an aluminium-7% silicon matrix (Figs. 4 and 5) is very much like that of specimens with a pure aluminium matrix; this is due to the fact that the proportional limit of the alloy employed was similar to that of the pure aluminium. The specimen with a matrix of aluminium-13% silicon showed an extremely interesting behaviour: the bulk of the specimen was composed of super-refined alloy of low proportional limit and high ductility (20%) while one external surface was composed of a brazing quality alloy (proportional limit: 9 kg mm^{-2}; 5% plastic deformation). After the fatigue test this latter alloy was only slightly cracked, without evidence of ribbon fracture, while the opposite surface of the specimen showed extensive matrix and ribbon fracture. This result clearly shows that, although the ribbon fracture determines the useful life of the composite, the fatigue processes leading to fracture are controlled by the matrix deformation.

The same conclusion has been reached by Toth [14] for fatigue in longitudinal boron filament reinforced 6061-Al alloy.

6. Fatigue results and discussion of transverse composites

6.1. Narrow ribbons

The results obtained on the fatigue behaviour of composites containing 4 mm wide ribbons, tested in the sense perpendicular to the principal ribbon axis (transverse composites) are presented in Table II and Fig. 6.

Figs. 7 and 8 show the difference in behaviour

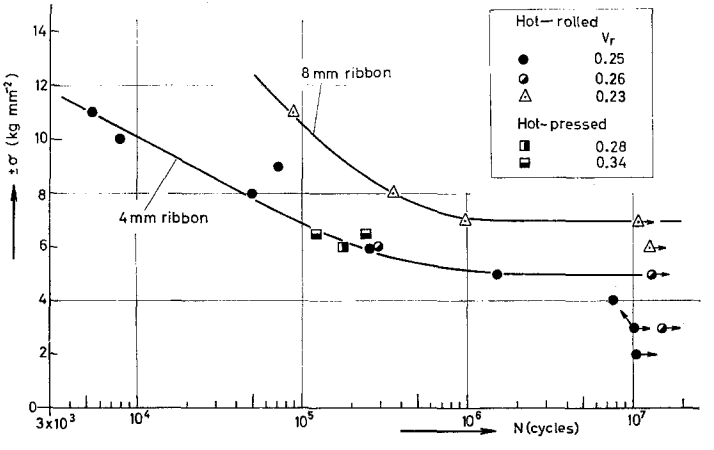

Figure 6 Number of cycles to "failure" as a function of alternating stress for transverse aluminium-steel ribbon composites.

TABLE II Results of fatigue tests in reverse bend at $\pm\sigma_F$ on hot-rolled transverse composites containing 4 mm wide ribbons in pure Al matrix

Test specimen Volume fraction of ribbons, V_r	Frequency (Hz)	$\pm\sigma_F$ (kg mm^{-2})	Number of cycles N ($\times 10^{-6}$)	$\pm\sigma$ deflection at the end of the fatigue test (kg mm^{-2})	Tensile strength after test σ_E (kg mm^{-2})	Tensile strength before test σ_C	σ_E/σ_C (%)
0.25	25	5.0	1.6	1.2	0.8	16.4	5
	10	8.0	0.05	2.4	4.5	,,	27
	10	11.0	0.005	2.9	0.9	,,	6
	10	10.0	0.007	2.4	1.3	,,	8
0.26	25	4.0	0.2	0.3	0.2	21.5	1
	25	3.0	11.8	3.0			
		to	10.6	4.6			
			15.1	5.0			
		6.0	0.28	3.8	3.3	21.5	15
0.25	25	2.0-	10.9	2.0			
		5.0	0.05	1.9	0.2	10.9	2
	25	3.0-	11.9	3.0			
		4.0	7.8	1.7			
0.23	25	3.0	0.2	small	0.3	7.6	4
0.25 annealed 410°C for 3 h	25	6.0	0.26	2.2	0.9	12.7	7
	10	9.0	0.07	2.3	1.1	12.7	8

of composites with $V_r = 0.25$ at high and low alternating stress levels, i.e., short and long lifetimes. At high stress levels, the failure progresses by matrix-ribbon splitting at ribbon ends, the initial cracks prolonging the ribbons along lines of lowest interfacial strength (Fig. 7). At lower stress levels the duration of the test is sufficient to lead to localized matrix cracking in the interior of the specimen following presumably on interfacial delamination, i.e., matrix crack initiation takes place predominantly at free surfaces, as in metals, and as previously observed by Hancock [18].

As in the longitudinal composites the delamination takes place preferentially along the matrix coating/matrix foil interface rather than along the matrix/ribbon interface. The stress build-up in the matrix in Fig. 8 has been sufficient to fracture one ribbon.

In contrast to the longitudinal composites there does not seem to be an effect of ribbon content on the fatigue limit, which at 10^7 cycles is about $\pm$ 5 kg mm^{-2} for all the specimens. This stress corresponds approximately to a plastic strain per cycle of the order of 0.1% calculated from a relation [10] analogous to Equation 1, i.e.,

$$\Delta e_p \sim \frac{2\sigma_F - (2\sigma_{ym}/E_m)[E_r V_r[1 - W_c/2W] + E_m(1 - V_r)]}{E_r V_r[1 - W_c/2W] + (\delta\sigma/\delta\epsilon)(1 - V_r)} \quad (2)$$

where the various terms have been defined previously.

The S/N curve for transverse composites indicates that there is a fatigue limit, in contrast to aluminium alloys whose fatigue resistance diminishes gradually with increasing number of cycles. At high stresses the curve resembles that of aluminium alloys with a gradual rise rather than an abrupt increase as is the case of the longitudinal composites and of course steel. The apparent invariance of the behaviour with V_r could be due to the fact that the ribbon width of 4 mm is close to the critical ribbon width measured in tension.

TABLE III Results of fatigue tests on hot-rolled transverse composites containing 8 mm wide ribbons in pure Al matrix

Volume fraction, V_r	Thickness (mm)	Stress $\pm \sigma_F$ (kg mm^{-2})	Number of cycles N	Observations
0.23	1.56	± 8.0	0.36×10^6	Clean fracture in centre of specimen (3 ribbons broken)
		± 7.0	0.96×10^6	Clean fracture in centre of specimen
		± 6.0 to ± 7.0	$> 12.5 \times 10^6$	Modulus constant
		± 7.0 to ± 8.0	$> 10.6 \times 10^6$	as above
		± 11.0	0.17×10^6	as above
			0.08×10^6	Clean fracture in centre of specimen

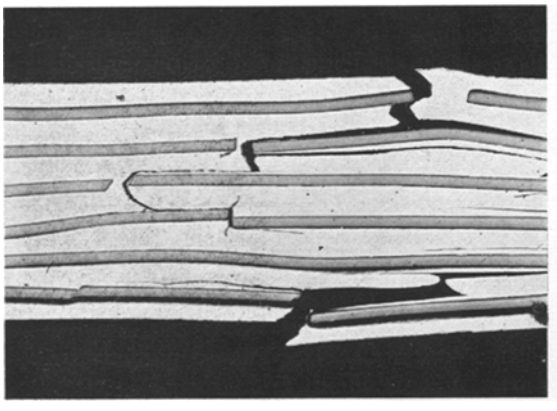

Figure 7 Transverse composite containing 4 mm ribbons; $V_r = 0.25$; tested at alternating stress level of $\pm$ 10 kg mm^{-2}. Structure at failure after 7×10^3 cycles ($\times 20$).

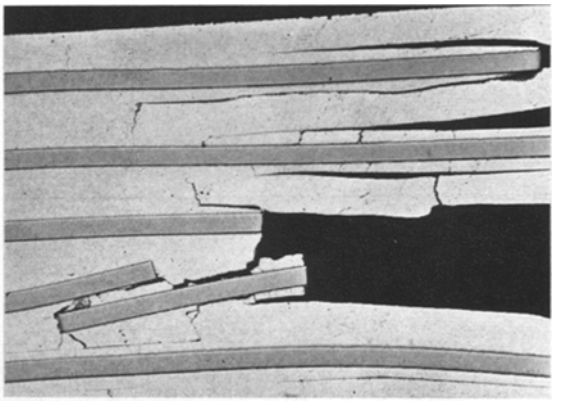

Figure 8 Transverse composite containing 4 mm ribbons; $V_r = 0.25$; tested at alternating stress level of $\pm$ 3 kg mm^{-2} for 1.19×10^7 cycles followed by 7.8×10^6 cycles at $\pm$ 4 kg mm^{-2}. Structure at failure showing matrix fatigue damage and ribbon fracture ($\times 40$).

6.2. Wide ribbons

The results for specimens containing 8 mm wide ribbons are presented in Table III and Fig. 6. The fatigue limit increases with increasing ribbon width but still corresponds to a critical plastic strain range of about 0.1%. Thus, although as in the case of the longitudinal composites the development of the fatigue damage is determined by the aluminium matrix, the limit is in part controlled by the ribbons.

In composites containing 8 mm wide ribbons the fatigue develops as follows.

During a test at a stress above the fatigue limit the first deformation is evident after $\sim 30\%$ of the total life of the specimen on the surfaces at regions corresponding to ribbon junctions in the external layers. After $\sim 50\%$ of the total life a localized deformation is apparent in the external steel ribbons at regions corresponding to ribbon junctions in the adjacent layer. During this period the effective modulus remains constant and continues to be, more or less, up to final rupture which follows closely on rupture of a surface ribbon at 90% of total life. The final fracture is made up of alternate broken and pulled-out ribbons.

The important point here is that there is no

gradual decrease of the modulus during the fatigue test even although matrix deformation is observed at a relatively early stage. The metallographic evidence indicates that this effect might be due to the fact that, in contrast to the longitudinal specimens and transverse specimens containing short ribbons no matrix-matrix or matrix-ribbon delamination is observed. This difference stems mainly from the fact that the latter specimens were fabricated from coated ribbons and matrix foils while the 8 mm ribbons were fabricated by rolling of uncoated ribbons and matrix foils. In addition of course, in contrast to the composites containing narrow ribbons the stress is more efficiently transferred to the wider 8 mm ribbons.

Fig. 9 is a photomicrograph of the fracture surface of the specimen which failed after 0.36×10^6 cycles at a stress level of $\pm$ 8 kg mm^{-2}. The clean break due to alternate ribbon fracture and pull out has taken place with little fatigue deformation in the matrix in the interior of the specimen. This is due to the fact that no delamination has taken place. Matrix fatigue deformation was also evident at other regions in the surface matrix layers.

Fig. 10 shows the partial propagation of a crack from one external surface in the specimen which underwent testing at increasing stresses. Some crack deflection along the ribbons is evident in the matrix, not along the steel-intermetallic or aluminium-intermetallic interfaces. Other regions in the external layers of the specimen between the final rupture (in grips) and the region of maximum stress (Fig. 10) also exhibit matrix cracking.

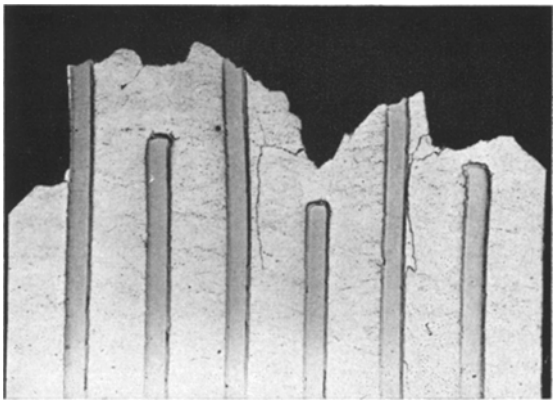

Figure 9 Transverse composite containing 8 mm ribbons; $V_r = 0.23$. Fracture surface after testing to 0.36×10^6 cycles at an alternating stress level of $\pm$ 8 kg mm^{-2} ($\times$40).

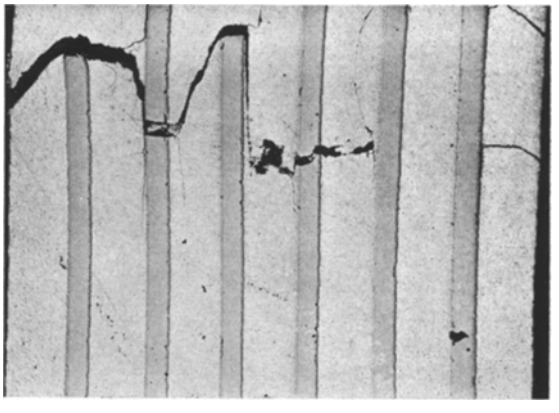

Figure 10 Transverse composite containing 8 mm ribbons; $V_r = 0.23$. Shows partial fatigue crack propagation in region away from main fracture which took place in the grips ($\times$40).

7. General discussion

7.1. Comparison with a high strength aluminium alloy

The results obtained for a 7075-T6 aluminium alloy are presented in Fig. 3. The test conditions were identical to those described for the composites and the fatigue limit at 10^7 cycles was $\pm$ 15 kg mm^{-2}, which is about the fatigue limit of a longitudinal composite containing 0.30 ribbon volume fraction. However, there is a marked difference in the fatigue behaviour of the two materials. The composite fatigue limit corresponds to the half-destruction of the specimen, whereas for the alloy the limit corresponds to complete fracture. The cracks in the composites propagate discontinuously in contrast to the catastrophic propagation in the alloy immediately following on the appearance of the first surface crack. This crack sensitivity, which was also exhibited by an alloy specimen containing a central hole, is one of the drawbacks of high-strength aluminium alloys which can be overcome by the incorporation of high-strength ribbons. Fig. 3 also shows that at high alternating stresses of the order of $\pm$ 25 kg mm^{-2}, composites with $V_r = 0.25$ are more resistant than the 7075-T6 alloy.

7.2. Effect of delamination on fatigue

The study of specimens fabricated on the one hand from uncoated ribbons and aluminium foil and on the other hand from ribbons coated with aluminium and aluminium foil has brought

to light an interesting difference in fatigue behaviour between the two.

In the transverse specimens containing wide ribbons the fabrication was carried out by simple hot-rolling of the steel ribbons and matrix foils, the bonding being assured by a metallurgical bond, with intermetallic formation between the steel and the aluminium. Upon fatigue testing the matrix cracks initiate on the free external surfaces and propagate to the ribbon interface without causing any delamination. With further stressing these original cracks cause some matrix cracking parallel to the ribbons and also ribbon fracture. The process continues till final failure takes place.

This relatively unhindered crack propagation is reminiscent of the 7075 aluminium alloy behaviour and, as with this alloy, some problem of composite failure in the grips was experienced. Since, in the case of the alloy this effect was put down to surface stress concentrations, it seems that the composites possessing little possibility of crack deflection are more sensitive to stress concentrations than the composites which exhibit some delamination perpendicular to the principal matrix crack direction.

All the longitudinal specimens and the transverse composites containing short ribbons (3 and 4 mm wide) discussed here were fabricated from coated ribbons and matrix foil. The steel-aluminium bond was assured during the coating step and the aluminium-aluminium bond during the hot-pressing or hot-rolling. As it turns out, this latter bond is often the weakest in the structure with the result that, during fatigue testing it can break down leading to delamination and loss of solidity of the composite.

However, if the aluminium-aluminium bond is not so weak as to break down early in the fatigue test, the presence of a low resistance plane perpendicular to the axis of propagation of matrix cracks can lead to high crack propagation resistance, i.e., the propagating matrix crack is deflected along the lines of weakest resistance. The consequence of this on the fatigue life of the composite is difficult to evaluate because going against the crack deflection property is the fact that matrix crack initiation can take place on the freshly created internal surfaces.

Thus, at present it is not possible to draw definite conclusions concerning the utility or not of having composites fabricated from coated ribbons. However, it is worth mentioning that in previous work [2] on the deformation mechanism in the steel ribbon composites the presence of the pre-coated layer reduced the effect of stress concentrations at ribbon extremities on the neighbouring ribbons.

8. Conclusions

1. The development of the fatigue deformation is controlled by the matrix in the case of both longitudinal and transverse composites.
2. The fatigue resistance (useful life) is determined for both longitudinal and transverse composites by the resistance of the steel ribbons.
3. The fatigue behaviour of the composites seems to be independent of the technique of fabrication, hot-pressing or hot-rolling.
4. The fatigue limit of longitudinal composites increases with increasing ribbon content.
5. The fatigue limit of transverse composites increases with increasing ribbon width because of more efficient transfer of the stress to the ribbons.
6. The use of a higher strength aluminium-silicon alloy matrix increases the composite fatigue resistance.
7. The use of pre-coated ribbons in the composite manufacture may be an interesting way to increase the resistance of the composite to fatigue crack propagation, due to delamination along the matrix/coating interface.

Acknowledgements

The author wishes to thank Miss R. Bode and Mr Ph. Reymond for assistance with the composite preparation and testing, Dr J. Rexer for helpful discussions and Péchiney-Ugine-Kuhlmann, Paris, for sponsoring the research programme.

References

1. E. ANDERSON, B. LUX, and C. CRUSSARD, *Revue de Métallurgie* (2) (1972) 165.
2. E. ANDERSON and R. BODE, "Failure Modes in Composites", Met. Soc. AIME, Boston, 1972.
3. P. M. SCOP and A. S. ARGON, *J. Comp. Materials* **1** (1967) 92; *ibid*, **3** (1969) 30.
4. J. HALPIN and R. L. THOMAS, *ibid* **2** (1968) 488.
5. P. E. CHEN and L. E. NIELSEN, *Kolloid-Z. und Z. für Polymere* **235** (1) (1969) 1174.
6. R. M. GRAY, "Metal Matrix Composites", Met. Soc. AIME Conf., 1969 (Pittsburg; DMIC Memo 243, 1969) p. 52.
7. P. J. E. FORSYTH, R. W. GEORGE, and D. A. RYDER, *Appl. Mat. Res.* **3** (1964) 223.
8. A. A. BAKER, *ibid* **5** (1966) 143.
9. *Idem, J. Mater. Sci.* **3** (1968) 412.

10. *Idem, Appl. Mat. Res.* **5** (1965) 210.
11. A. VARSCHAVSKY and P. TAMAYO, *J. Mater. Sci.* **4** (1969) 653.
12. K. C. ANTHONY and W. H. CHANG, *Trans. ASM* **61** (1968) 550.
13. H. SHIMIZU and J. F. DOLOWY, JUN., "Composite Materials: Testing and Design", ASTM STP 460 (1969) p. 192.
14. I. J. TOTH, "Composite Materials: Testing and Design", ASTM STP 460 (1969) p. 236.
15. J. R. HANCOCK, AGARD Conf. on "Composite Materials", Paris 1970, paper 14.
16. K. G. KREIDER and G. R. LEVANT, SAMPE Conf. on "Advanced Fibrous Composites", **10** (1966) F-1.
17. A. A. BAKER, D. M. BRADDICK, and P. W. JACKSON *J. Mater. Sci.* **7** (1972) 747.
18. J. R. HANCOCK, "Composite Materials: Testing and Design", Second Conference, ASTM STP 497 (1972) p. 483.

Received 2 November and accepted 8 December 1972.